October, 1993] © *1993 The Chemical Society of Japan* *Bull. Chem. Soc. Jpn.,* ***66****, 2847—2853(1993)* 2847

Crystal Structures of the Room-Temperature Phase of 4,4″-Difluoro-*p*-terphenyl and 4,4‴-Difluoro-*p*-quaterphenyl

Hideki Saitoh, Kazuya Saito,* Yasuhisa Yamamura, Haruo Matsuyama, Koichi Kikuchi, Masahiko Iyoda, and Isao Ikemoto*
Department of Chemistry, Faculty of Science, Tokyo Metropolitan University, Hachioji, Tokyo 192-03

(Received May 6, 1993)

4,4″-Difluoro-*p*-terphenyl and 4,4‴-difluoro-*p*-quaterphenyl were synthesized and their crystal structures were determined at room temperature. These are isostructural to *p*-terphenyl and *p*-quaterphenyl, respectively. Some "disorder" in the inner benzene ring orientation was detected and resolved by the split-atom method. A rigid-body librational analysis of each benzene ring around the long molecular axis was performed. A rough estimate of the barrier height of the planar conformation for 4,4″-difluoro-*p*-terphenyl was obtained as being about 1 kJ mol^{-1}. The results are compared with the properties of *p*-terphenyl and *p*-quaterphenyl, and the effect of fluorine-substitution on the molecular properties is discussed in relation to the low-temperature phase transitions.

Compounds of the so-called *p*-polyphenyls have attracted much attention owing to their molecular flexibility. While the molecules are twisted in the gaseous and liquid states due to a repulsion between the *ortho*-hydrogen atoms,[1—7] those of, at least, the first three members (biphenyl,[8—13] *p*-terphenyl[14,15] and *p*-quaterphenyl[16]) are seemingly planar in the crystal form at room temperature. The crystals undergo a structural phase transition at low temperature,[17] below which the molecules resume the twisted conformation.[18—21] The properties of the phase transitions are, however, much different from each other. The transition in biphenyl (at 40.4 K)[22,23] is of the displacive type associated with soft-modes.[24] On the other hand, the transitions in *p*-terphenyl (at 193.5 K)[25,26] and *p*-quaterphenyl (at 233.0 K)[27] are of the order-disorder type.[28—35] It is commonly accepted that the transitions result from the delicate balance between the intra- and the inter-molecular interactions.[17,36]

Since the "twist" transition is common in crystalline *p*-polyphenyls, it is desired to establish a unified description. The number of systems available is three, which seems to be too small for such a purpose. An attempt to increase the number was made by one of the authors by modifying the biphenyl molecule.[37] The result of a search for a possible "twist" transition in crystalline 4,4′-difluorobiphenyl was negative, despite having essentially the same crystal structure as for biphenyl;[38,39] this was interpreted as being due to the too strong stability of the planar conformation, due to the extended π orbital.[37,40] This interpretation was later confirmed by a librational analysis of the benzene ring.[38] Namely, the fluorine-substitution enhances the stability of the planar molecular conformation, thus lowering the "twist" transition temperature. The fluorine substitution on larger *p*-polyphenyls, therefore, seems to promise an increase in the number of systems that can show a "twist" transition, as long as they crystallize in the same manner as the corresponding unsubstituted molecules. These situations led us to start studying 4,4″-difluoro-*p*-terphenyl (DFTP) and 4,4‴-difluoro-*p*-quaterphenyl (DFQP). Prior to an additional study of their low-temperature behaviors, structure analyses were carried out in order to determine whether they have essentially the same crystal structure as the corresponding compounds. In this paper, the synthesis is briefly described, and detailed descriptions are given concerning their crystal structure, especially some kind of "disorder". The results are compared with the crystal properties of *p*-terphenyl and *p*-quaterphenyl in relation to the properties of possible "twist" transitions.

Experimental

Samples. DFTP: *p*-Fluorophenylmagnesium bromide was prepared in tetrahydrofuran (THF) from magnesium shavings and *p*-bromofluorobenzene in a three-necked flask equipped with a pressure-equalizing dropping funnel, a condenser and a magnetic stirrer. To the solution was added dry zinc chloride dissolved in THF at room temperature under a nitrogen atmosphere. After stirring for 1 h at room temperature, first bis(triphenylphosphine)nickel(II) chloride was added and then *p*-dibromobenzene in THF was slowly added. After the solution had been stirred for 10 h at room temperature, 2 mol dm^{-3} hydrochloric acid was added. The mixture was extracted twice with benzene. The combined organics were washed with water, dried over $MgSO_4$, and filtered; the solvent was then removed to give a solid. After the solid had been eluted through an Al_2O_3 column with benzene, the solvent was evaporated to give DFTP (66% yield). The compound was further purified by gel-permeation chromatography (GPC) using a JAI LC-08 liquid chromatograph with two JAIGEL-1H columns (20 ×600 mm) with chloroform used as the eluent. Melting point 214—215 °C; Mass m/z 266 (M^+).

DFQP: DFQP was synthesized in a similar manner (60% yield) as that for DFTP. However, 4,4′-dibromobiphenyl was used instead of *p*-dibromobenzene as the starting compound. The resulting crude DFQP was washed with hot chloroform and a hot toluene–chloroform mixture (1 : 1) in order to remove any soluble by-products (difluorobiphenyl and DFTP). The remaining solid was analyzed by mass spectrometry, showing that the solid mainly comprised DFQP with a small amount of impurity, difluoro-*p*-quinquaphenyl. Melting point, not determined; Mass m/z 342 (M^+).

Crystals of DFTP, DFQP, and *p*-terphenyl (Nacalai Chemicals, Ltd.) were prepared by recrystallization from acetone, chloroform–dichloromethane and toluene solutions, respectively. The densities of the crystals were not measured.

Data Collection and Computation. All X-ray measurements were made using an automatic four-circle diffractometer (Mac Science, MXC18). The radiation used for the measurement was graphite-monochromated Mo $K\alpha$ (λ=0.71069 Å). The sample size was 0.43×0.35×0.06 mm^3 for DFTP (0.45×0.38×0.05 mm^3 for DFQP). The unit cell dimensions were determined from 17 (23) reflections in the range of $22° < 2\theta < 30°$ ($18° < 2\theta < 30°$). The intensity data were measured with the 2θ–ω scan technique over all angles. The scan rate and the scan width were 4(8) ° min^{-1} in ω-axis and $\Delta\omega = 1.30° + 0.40° \tan\theta$ ($\Delta\omega = 1.30° + 0.25° \tan\theta$). The maximum value of $(\sin\theta)/\lambda$ and h, k, and l were 0.704 Å^{-1}, $-11 \leq h \leq 11$, $0 \leq k \leq 8$, and $0 \leq l \leq 19$ (0.756 Å^{-1}, $-11 \leq h \leq 11$, $0 \leq k \leq 8$, $0 \leq l \leq 27$). Three standard reflections were measured at an interval of 100 reflections. The variations were random and small (<1.4%). The intensity data were not corrected for absorption effects, because of the small linear absorption coefficient. The criterion for ignoring data in the refinement was $|F_o| < 3.0\sigma(|F_o|)$. The systematic absence of reflections revealed the space group $P2_1/a$ for both compounds. This was later confirmed by a successful structure solution and a least-square refinement. Parameter refinements were carried out by the block-diagonal least-squares method. The atomic and anomalous scattering factors were taken from the literature.[41] All computations, except for the structure solution, were carried out using the UNICS III program system.[42] The structure was solved by the direct method with SHELXS-86.[43] All of the hydrogen atoms were located in difference syntheses and refined isotropically, except for the split atoms in DFQP. No secondary extinction corrections were applied. ORTEP II[44] was used to produce crystal-structure illustrations.

Table 1. Crystal Data and Details of Refinements

	DFTP	DFQP
Molecular formula	$C_{18}H_{12}F_2$	$C_{24}H_{16}F_2$
Formula weight	266.28	342.37
Crystal system	Monoclinic	Monoclinic
Space group	$P2_1/a$	$P2_1/a$
a/Å	7.874(2)	7.910(1)
b/Å	5.748(1)	5.693(1)
c/Å	14.159(3)	18.395(2)
β/°	93.31(2)	96.59(1)
V/Å^3	639.8(2)	822.9(2)
Z	2	2
D_x/Mg m^{-3}	1.38	1.38
μ(Mo $K\alpha$)/cm^{-1}	0.936	0.890
$F(000)$	276	356
No. of data	2113	3320
No. of data used in refinement [$\lvert F_o\rvert > 3.0\sigma(\lvert F_o\rvert)$]	1289	1217
Refinement assuming non-split atom		
No. of variables	116	151
R and wR	0.070, 0.072	0.102, 0.066
S	2.71	2.14
$(\Delta/\sigma)_{\max}$	0.0003	0.0003
Density in difference synthesis/e Å^{-3}	−0.35—0.18	−0.41—0.36
Refinment assuming split atom		
No. of variables	142	195
R and wR	0.063, 0.061	0.090, 0.057
S	2.28	1.92
$(\Delta/\sigma)_{\max}$	0.074	0.075
Density in difference synthesis/e Å^{-3}	−0.33—0.18	−0.33—0.29

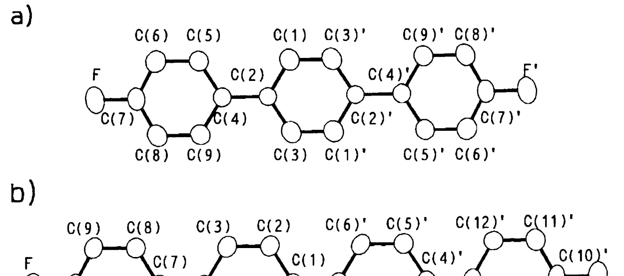

Fig. 1. Numbering scheme for DFTP (a) and DFQP (b) molecules. The hydrogen atoms are not shown because of their trivial notation.

Results and Discussion

The structure was successfully solved for both DFTP and DFQP by the direct method. The function $\Sigma w(|F_o| - |F_c|)^2$ was minimized for refinements, where $w = [\sigma^2(|F_o|) + 0.0002|F_o|^2]^{-1}$ for DFTP, and $w = [\sigma^2(|F_o|) + 0.0001|F_o|^2]^{-1}$ for DFQP. The details concerning the refinements are summarized in Table 1. The resulting positional and thermal parameters[45] are tabulated in Tables 2 and 3 for DFTP and DFQP, respectively; the numbering schemes are given in Fig. 1. The crystal structures viewed along the *b*-axis are shown in Fig. 2. In the crystals of both compounds, since the molecules are located on an inversion center, half of the molecule is crystallographically independent. The long molecular axes of both compounds are nearly in the *ac* plane. The crystals are isostructural to those of the high-temperature phase of the corresponding unsubstituted compounds, *p*-terphenyl[14,15] and *p*-quaterphenyl.[16] The fluorine-substituted *p*-polyphenyls are, therefore, the appropriate objects for a unified understanding of the "twist" transitions. Indeed, the molecular packing in the *ab* plane is essentially the same among *p*-terphenyl, DFTP and DFQP, as can be clearly seen in Fig. 3.

The bond lengths and angles are given in Tables 4 and 5 for DFTP and DFQP, respectively. Sideviews

Table 2. Fractional Atomic Coordinates and Equivalent Isotropic Thermal Factors of DFTP Obtained by the Non-Split Atom Analysis (Left) and the Split Atom Analysis (Right)

Atom	$10^4 \cdot x$	$10^4 \cdot y$	$10^4 \cdot z$	$B_{eq}^{a)}/\text{Å}^2$	Atom	$10^4 \cdot x$	$10^4 \cdot y$	$10^4 \cdot z$	$B_{eq}^{a)}/\text{Å}^2$
F	−2173(2)	−15(2)	4756(1)	5.66(4)	F	−2171(2)	−14(2)	4757(1)	5.69(3)
C(1)	−979(3)	−1717(4)	339(1)	5.15(6)	C(1A)	−718(4)	−1911(6)	402(2)	3.80(9)
					C(1B)	−1189(4)	−1532(6)	283(2)	3.17(7)
C(2)	−439(2)	4(3)	963(1)	2.63(4)	C(2)	−440(2)	4(2)	964(1)	2.63(3)
C(3)	553(3)	1717(4)	598(1)	5.13(7)	C(3A)	282(4)	1936(6)	538(2)	3.52(8)
					C(3B)	776(4)	1515(6)	646(2)	3.03(7)
C(4)	−904(2)	−1(3)	1969(1)	2.76(4)	C(4)	−901(2)	0(3)	1969(1)	2.74(3)
C(5)	−1868(3)	−1778(4)	2334(1)	3.74(5)	C(5)	−1860(2)	−1780(3)	2333(1)	3.71(4)
C(6)	−2298(3)	−1802(4)	3268(1)	4.20(5)	C(6)	−2294(2)	−1804(3)	3269(1)	4.23(5)
C(7)	−1752(2)	−13(4)	3842(1)	3.71(5)	C(7)	−1748(2)	−13(3)	3842(1)	3.74(4)
C(8)	−806(3)	1786(4)	3526(1)	4.32(6)	C(8)	−808(2)	1787(3)	3526(1)	4.26(5)
C(9)	−387(3)	1791(4)	2588(1)	3.83(5)	C(9)	−389(2)	1788(3)	2588(1)	3.79(4)
Atom	$10^3 \cdot x$	$10^3 \cdot y$	$10^3 \cdot z$	$B_{iso}/\text{Å}^2$	Atom	$10^3 \cdot x$	$10^3 \cdot y$	$10^3 \cdot z$	$B_{iso}/\text{Å}^2$
H(C1)	−192(3)	−292(4)	53(1)	7.6(6)	H(C1A)	−119(4)	−342(6)	64(2)	4.4(7)
					H(C1B)	−210(3)	−262(4)	47(2)	2.6(6)
H(C3)	119(3)	293(5)	102(1)	8.1(7)	H(C3A)	49(4)	338(5)	91(2)	3.7(7)
					H(C3B)	136(3)	263(5)	107(2)	3.2(6)
H(C5)	−237(2)	−305(3)	193(1)	4.6(4)	H(C5)	−225(2)	−309(3)	194(1)	4.8(4)
H(C6)	−304(3)	−297(4)	349(1)	5.6(5)	H(C6)	−298(2)	−298(3)	350(1)	5.9(4)
H(C8)	−43(3)	302(4)	397(1)	6.0(5)	H(C8)	−40(2)	302(3)	395(1)	5.9(4)
H(C9)	39(3)	302(4)	239(1)	5.6(5)	H(C9)	24(2)	304(3)	237(1)	5.0(4)

a) $B_{eq}=(4/3)\cdot(B_{11}\boldsymbol{a}\cdot\boldsymbol{a}+B_{12}\boldsymbol{a}\cdot\boldsymbol{b}+B_{13}\boldsymbol{a}\cdot\boldsymbol{c}+\cdots)$.

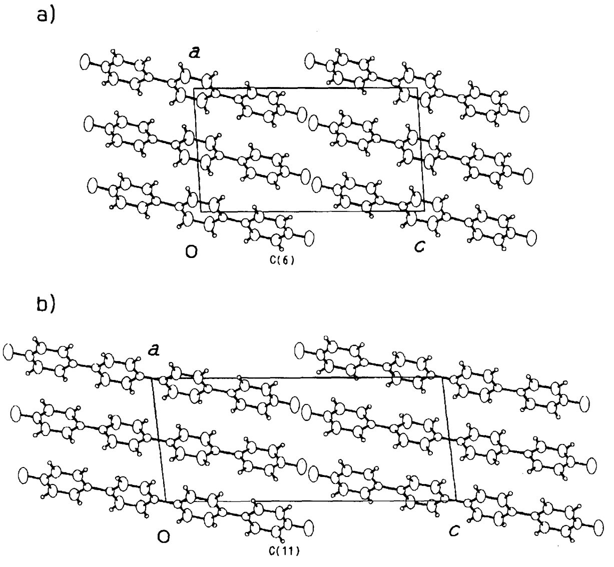

Fig. 2. Crystal structures obtained by the non-split atom analysis on DFTP (a) and DFQP (b) viewed along the *b*-axis. Thermal ellipsoids of the fuorine and carbon atoms show the region of 50% probability.

of the molecules are shown in Fig. 4. Both molecules are seemingly almost planar (within 0.03 Å for DFTP and 0.02 Å for DFQP). The thermal ellipsoids of the off-center carbon atoms (C(1) and C(3)) on the central benzene ring of DFTP are, however, abnormally elongated along the molecular plane normal. A similar trend can also be recognized for those of DFQP. This information suggest the existence of some type of "disorder" in the orientation of the inner benzene ring(s),

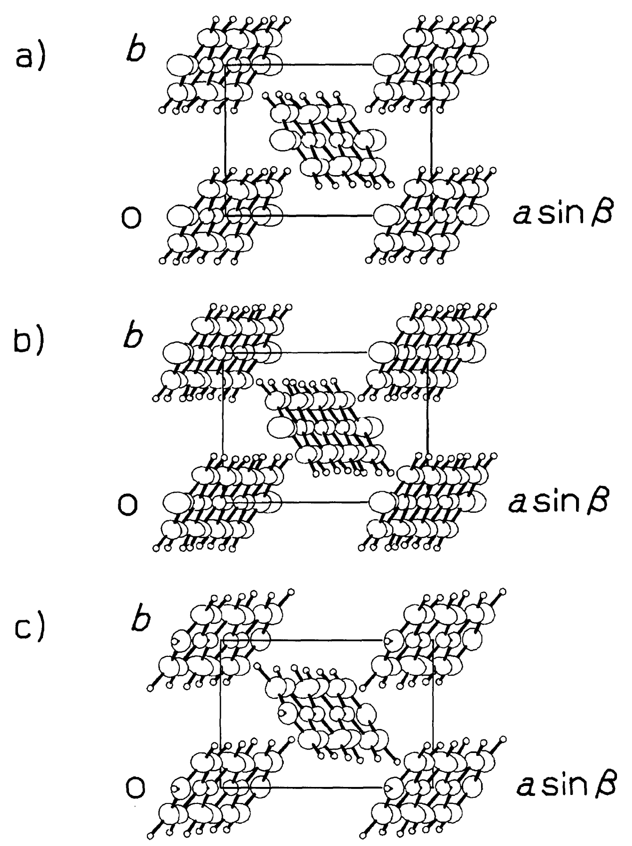

Fig. 3. Crystal structures obtained by the non-split atom analysis on DFTP (a), DFQP (b), and *p*-terphenyl (c) viewed along the *c*-axis.

Table 3. Fractional Atomic Coordinates and Equivalent Isotropic Thermal Factors of DFQP Obtained by the Non-Split Atom Analysis (Left) and the Split Atom Analysis (Right)

Atom	$10^4 \cdot x$	$10^4 \cdot y$	$10^4 \cdot z$	$B_{eq}^{a)}/Å^2$	Atom	$10^4 \cdot x$	$10^4 \cdot y$	$10^4 \cdot z$	$B_{eq}^{a)}/Å^2$
F	−2191(3)	−13(5)	4811(1)	5.8(1)	F	−2191(3)	−15(4)	4812(1)	5.8(1)
C(1)	−184(4)	3(8)	389(1)	2.3(1)	C(1)	−190(3)	−2(7)	387(1)	2.4(1)
C(2)	398(5)	1772(8)	867(2)	4.2(1)	C(2A)	208(8)	1750(14)	783(3)	3.8(2)
					C(2B)	545(7)	1726(12)	931(3)	3.0(2)
C(3)	73(5)	1761(8)	1592(2)	4.4(1)	C(3A)	31(8)	1925(11)	1519(3)	3.2(2)
					C(3B)	84(9)	1515(14)	1662(3)	4.1(2)
C(4)	−863(4)	6(7)	1879(2)	2.4(1)	C(4)	−863(3)	−6(6)	1879(1)	2.5(1)
C(5)	−1447(5)	−1737(8)	1394(2)	4.4(1)	C(5A)	−1259(7)	−1985(10)	1437(3)	2.3(1)
					C(5B)	−1644(7)	−1470(12)	1345(3)	3.4(2)
C(6)	−1105(5)	−1744(8)	672(2)	4.2(1)	C(6A)	−852(8)	−1807(12)	745(3)	3.2(2)
					C(6B)	−1323(6)	−1702(12)	608(3)	2.5(1)
C(7)	−1215(4)	−7(7)	2656(1)	2.5(1)	C(7)	−1212(3)	−1(6)	2654(1)	2.5(1)
C(8)	−628(5)	1786(7)	3136(2)	3.8(1)	C(8)	−638(4)	1771(6)	3135(2)	3.8(1)
C(9)	−946(5)	1814(8)	3860(2)	4.0(1)	C(9)	−950(4)	1806(7)	3862(2)	4.1(1)
C(10)	−1856(4)	8(8)	4101(2)	3.6(1)	C(10)	−1858(4)	−2(7)	4101(1)	3.5(1)
C(11)	−2468(5)	−1805(8)	3661(2)	4.0(1)	C(11)	−2470(4)	−1795(7)	3661(2)	3.9(1)
C(12)	−2150(5)	−1791(7)	2937(2)	3.6(1)	C(12)	−2137(4)	−1785(6)	2936(2)	3.6(1)
Atom	$10^3 \cdot x$	$10^3 \cdot y$	$10^3 \cdot z$	$B_{iso}/Å^2$	Atom	$10^3 \cdot x$	$10^3 \cdot y$	$10^3 \cdot z$	$B_{iso}/Å^2$
H(C2)	114(5)	289(8)	71(2)	8.1(12)	H(C2A)	67(6)	338(10)	65(3)	3.1
					H(C2B)	150(6)	255(9)	75(3)	3.1
H(C3)	61(4)	289(7)	190(2)	6.6(10)	H(C3A)	46(6)	327(10)	187(3)	3.1
					H(C3B)	72(6)	231(9)	187(3)	3.1
H(C5)	−192(4)	−304(7)	156(2)	5.6(9)	H(C5A)	−145(6)	−356(10)	163(3)	3.1
					H(C5B)	−237(6)	−274(9)	148(3)	3.1
H(C6)	−159(4)	−301(7)	36(2)	5.6(10)	H(C6A)	−112(6)	−337(10)	41(3)	3.1
					H(C6B)	−207(6)	−271(9)	27(3)	3.1
H(C8)	6(4)	299(6)	297(2)	3.9(8)	H(C8)	2(3)	301(5)	297(1)	3.7(7)
H(C9)	−44(4)	309(7)	423(2)	6.2(10)	H(C9)	−47(3)	308(6)	422(2)	6.1(9)
H(C11)	−322(4)	−305(7)	385(2)	6.2(10)	H(C11)	−311(4)	−313(6)	386(2)	6.9(9)
H(C12)	−264(4)	−301(6)	264(2)	4.3(8)	H(C12)	−258(3)	−295(5)	263(1)	3.5(7)

a) $B_{eq}=(4/3)\cdot(B_{11}\boldsymbol{a}\cdot\boldsymbol{a}+B_{12}\boldsymbol{a}\cdot\boldsymbol{b}+B_{13}\boldsymbol{a}\cdot\boldsymbol{c}+\cdots)$.

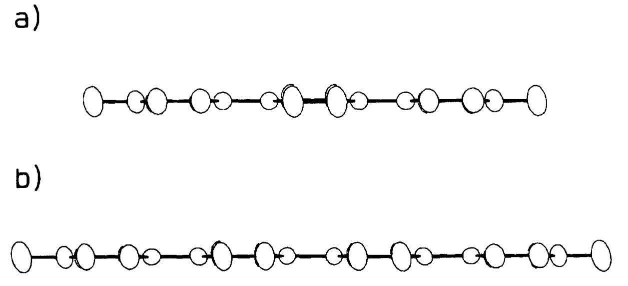

Fig. 4. Sideviews of DFTP (a) and DFQP (b) molecules obtained by the non-split atom analysis. The hydrogen atoms are not shown for clarity.

i.e., the conformational "disorder". In the case of *p*-terphenyl, the same type of disorder was detected and successfully resolved by assuming two central benzene rings having an opposing conformation with respect to the outer rings.[15)] Indeed, it has been widely believed that this disorder is a direct consequence of the order-disorder transition at 193.5 K.[15,17)]

Attempts to refine the structure were therefore carried out assuming the "disordered" inner benzene rings for both compounds, though such an analysis has not yet been made for *p*-quaterphenyl.[16)] The off-center carbon atoms of the inner benzene rings were split into two with equal occupancy. The relating hydrogen atoms were also split. The initial coordinates for DFTP were obtained from the coordinates of the corresponding atoms in *p*-terphenyl.[15)] Those for DFQP were generated while taking into account the results of a split-atom analysis of DFTP and the structure of the low-temperature phase of *p*-quaterphenyl.[21)] The weighting functions were the same as those used in the refinements assuming non-split atoms. The details concerning the refinements are summarized in Table 1. The reductions in the *R*-factors were about 1 per cent, and were significant in both cases. The same procedure was applied to the present reflection data for *p*-terphenyl[46)] for the sake of a comparison. The result was also successful. The new result, that the inner rings in DFQP can be split, suggests that a similar analysis is applicable, even for *p*-quaterphenyl, because the splitting of the atoms is larger than in the case of DFQP.

The positional and thermal parameters obtained after the split-atom analysis are tabulated in Tables 2 and 3 for DFTP and DFQP, respectively.[45)] The bond lengths and angles[45)] are within reasonable ranges. The two

Table 4. Bond Lengths (l) and Bond Angles (θ) of DFTP Obtained by the Non-Split Atom Analysis

Bond	l/Å	Bond	l/Å	Bond	l/Å
F–C(7)	1.354(2)	C(4)–C(9)	1.397(3)	C(1)–H(C1)	1.06(2)
C(1)–C(2)	1.378(3)	C(5)–C(6)	1.384(3)	C(3)–H(C3)	1.03(2)
C(1)–C(3)′	1.387(3)	C(6)–C(7)	1.365(3)	C(5)–H(C5)	0.99(2)
C(2)–C(3)	1.377(3)	C(7)–C(8)	1.365(3)	C(6)–H(C6)	0.95(2)
C(2)–C(4)	1.491(2)	C(8)–C(9)	1.387(3)	C(8)–H(C8)	0.98(2)
C(4)–C(5)	1.390(3)			C(9)–H(C9)	0.98(2)
Angle	**θ/°**	**Angle**	**θ/°**	**Angle**	**θ/°**
C(2)–C(1)–C(3)′	122.1(2)	C(2)–C(4)–C(5)	121.7(1)	F–C(7)–C(6)	118.9(2)
C(2)–C(1)–H(C1)	119.8(11)	C(2)–C(4)–C(9)	121.3(2)	F–C(7)–C(8)	118.8(2)
C(3)′–C(1)–H(C1)	117.3(11)	C(5)–C(4)–C(9)	117.0(1)	C(6)–C(7)–C(8)	122.3(2)
C(1)–C(2)–C(3)	115.7(2)	C(4)–C(5)–C(6)	122.1(2)	C(7)–C(8)–C(9)	118.7(2)
C(1)–C(2)–C(4)	121.9(2)	C(4)–C(5)–H(C5)	122.6(10)	C(7)–C(8)–H(C8)	119.2(12)
C(3)–C(2)–C(4)	122.4(2)	C(6)–C(5)–H(C5)	115.2(11)	C(9)–C(8)–H(C8)	122.1(12)
C(2)–C(3) –C(1)′	122.3(2)	C(5)–C(6)–C(7)	118.4(2)	C(4)–C(9)–C(8)	121.5(2)
C(2)–C(3)–H(C3)	122.0(12)	C(5)–C(6)–H(C6)	120.6(11)	C(4)–C(9)–H(C9)	120.7(11)
C(1)′–C(3)–H(C3)	115.0(12)	C(7)–C(6)–H(C6)	120.8(11)	C(8)–C(9)–H(C9)	117.5(10)

Table 5. Bond Lengths (l) and Bond Angles (θ) of DFQP Obtained by the Non-Split Atom Analysis

Bond	l/Å	Bond	l/Å	Bond	l/Å
F–C(10)	1.363(4)	C(5)–C(6)	1.385(5)	C(2)–H(C2)	0.93(4)
C(1)–C(1)′	1.492(4)	C(7)–C(8)	1.395(5)	C(3)–H(C3)	0.93(4)
C(1)–C(2)	1.381(5)	C(7)–C(12)	1.391(5)	C(5)–H(C5)	0.90(4)
C(1)–C(6)	1.371(6)	C(8)–C(9)	1.383(5)	C(6)–H(C6)	0.97(3)
C(2)–C(3)	1.387(5)	C(9)–C(10)	1.358(6)	C(8)–H(C8)	0.95(3)
C(3)–C(4)	1.383(6)	C(10)–C(11)	1.365(6)	C(9)–H(C9)	1.05(4)
C(4)–C(5)	1.378(5)	C(11)–C(12)	1.385(5)	C(11)–H(C11)	1.01(4)
C(4)–C(7)	1.487(4)			C(12)–H(C12)	0.94(3)
Angle	**θ/°**	**Angle**	**θ/°**	**Angle**	**θ/°**
C(2)–C(1)–C(6)	116.1(3)	C(4)–C(5)–C(6)	122.3(4)	C(8)–C(9)–C(10)	117.8(4)
C(2)–C(1)–C(1)′	121.7(4)	C(4)–C(5)–H(C5)	119.4(22)	C(8)–C(9)–H(C9)	122.9(20)
C(6)–C(1)–C(1)′	122.2(3)	C(6)–C(5)–H(C5)	117.5(22)	C(10)–C(9)–H(C9)	119.1(20)
C(1)–C(2)–C(3)	121.7(4)	C(1)–C(6)–C(5)	122.2(4)	F–C(10)–C(9)	119.2(3)
C(1)–C(2)–H(C2)	118.7(25)	C(1)–C(6)–H(C6)	120.2(20)	F–C(10)–C(11)	117.8(4)
C(3)–C(2)–H(C2)	119.2(25)	C(5)–C(6)–H(C6)	117.6(21)	C(9)–C(10)–C(11)	123.0(3)
C(2)–C(3)–C(4)	122.4(4)	C(4)–C(7)–C(8)	121.3(3)	C(10)–C(11)–C(12)	118.3(4)
C(2)–C(3)–H(C3)	117.9(23)	C(4)–C(7)–C(12)	121.8(3)	C(10)–C(11)–H(C11)	120.7(20)
C(4)–C(3)–H(C3)	119.4(23)	C(8)–C(7)–C(12)	116.9(3)	C(12)–C(11)–H(C11)	120.8(20)
C(3)–C(4)–C(5)	115.3(3)	C(7)–C(8)–C(9)	122.3(4)	C(7)–C(12)–C(11)	121.7(3)
C(3)–C(4)–C(7)	122.5(3)	C(7)–C(8)–H(C8)	119.5(19)	C(7)–C(12)–H(C12)	121.7(20)
C(5)–C(4)–C(7)	122.2(3)	C(9)–C(8)–H(C8)	118.1(19)	C(11)–C(12)–H(C12)	116.6(20)

inner benzene rings are almost planar within 0.005 and 0.006 Å for DFTP, and 0.07 and 0.08 Å for DFQP. The dihedral angles between two benzene rings with different conformations are 22.6(1)° and 15.6(2)°, for DFTP and DFQP, respectively. The dihedral angle for *p*-terphenyl obtained in the present analysis[46] is 26.0(2)°, and is in favorable agreement with the previous data (26.6°),[15] though the treatment of the split-atom analysis was somewhat different. The dihedral angle in DFTP is smaller than that in *p*-terphenyl. This is also the case for DFQP and *p*-quaterphenyl if the dihedral angle in DFQP and that between the inner benzene rings in the low-temperature phase of *p*-quaterphenyl[21] are compared. Thus, the fluorine-substitution enhances the stability of the planar conformation.

To obtain more details concerning the effect of fluorine-substitution on the libration of the benzene ring about the long molecular axis, a rigid-body librational analysis[47,48] was carried out while assuming that the inner benzene ring is a rigid body. The hydrogen atoms were not included in the analysis. The results of the rigid-body librational analysis of each ring are compared in Table 6. The librational amplitudes of the inner benzene ring about the long molecular axis are 87 (°)^2 and 92 (°)^2 in the split-atom analysis for DFTP and DFQP, respectively, and are of usual magnitude, as compared with the anomalously large values [250 (°)^2 and 187 (°)^2] in the non-split-atom analysis. This supports the validity of the present treatment of the "disorder".

The potential barrier height at the planar confor-

Table 6. Librational Amplitudes of the Inner Benzene Ring around the Long Molecular Axis ($<\Omega^2>$) at Room Temperature

	$<\Omega^2>/(°)^2$	
	Non-split atom analysis	Split atom analysis
DFTP	250(12)	87(12)
p-Terphenyl[a)]	270(9)	47(9)
DFQP	187(13)	92(25)
p-Quaterphenyl[b)]	178(5)	—

a) Present data.[46)] The previous results[15)] are 260(8) and 53(8) $(°)^2$.
b) Ref. 16.

mation in crystalline DFTP was estimated following Baudour.[49)] The resulting barrier height is about 1 kJ mol^{-1} or smaller. Since this value shows that the barrier is smaller than the thermal energy at room temperature, the estimated barrier height has a large uncertainty. The height is, however, definitely much smaller compared with 4.57 kJ mol^{-1} in *p*-terphenyl.[32,49)] This fact also supports the enhanced planarity in fluorine-substituted *p*-polyphenyls.

All of the features concerning the fluorine-substitution revealed in the present study for DFTP can be readily understood if we assume a quartic function as a potential function for the central benzene ring rotation in the crystal. The coefficient of the second-order term is negative, and that of the fourth-order term positive, since there is a barrier for the planar conformation. The third-order term is ignored for simplicity. The intermolecular force that favors the planar molecular conformation is little affected, since the molecular packing in the *ab* plane is essentially the same. It is, therefore, reasonable to suppose that the change in the libtational motion is solely due to the change in the intramolecular potential. Since the potential function far from the planar conformation is only slightly affected by the fluorine-substitution, because of the similar *ortho*-hydrogen repulsion and the negligible π conjugation, the enhanced stability of the planar conformation is equivalent to the increase in the coefficient of the second-order term, i. e., the decrease in the absolute value of the negative second-order coefficient, leading to a decrease in the difference between the maximum and minimum. In the case of a quartic function of double-minimum, the decrease in the maximum automatically corresponds to a reduction in the location of the minimum. In addition, the effective force constant at the minimum decreases with decreasing the barrier height, resulting in the increased "apparent" amplitute of the librational motion. A unified theory[50,51)] for a structural phase transition (assuming a quartic function as the one-particle potential) predicts a change in the nature of the phase transition from order-disorder type to the displacive type with decreasing the barrier height if the interparticle coupling is unchanged. Although the barrier height cannot be estimated for DFQP, the essential feature of the one-particle potential is the same. The low-temperature behaviors of DFTP and DFQP are therefore very interesting. A study along this line is in progress in this laboratory.

References

1) O. Bastiansen, *Acta Chem. Scand.*, **3**, 408 (1949).
2) H. Suzuki, *Bull. Chem. Soc. Jpn.*, **32**, 1340 (1959).
3) J. Dale, *Acta Chem. Scand.*, **11**, 640 (1957).
4) J. Dale, *Acta Chem. Scand.*, **11**, 650 (1957).
5) V. J. Eaton and D. Steele, *J. Chem. Soc., Faraday Trans. 2*, **69**, 1601 (1973).
6) A. J. Grumadas, D. P. Poshkus, and A. V. Kiselev, *J. Chem. Soc, Faraday Trans. 2*, **75**, 1398 (1979).
7) A. J. Grumadas, D. P. Poshkus, and A. V. Kiselev, *J. Chem. Soc, Faraday Trans. 2*, **78**, 2013 (1982).
8) G. L. Clark and L. W. Pickett, *J. Am. Chem. Soc.*, **53**, 167 (1931).
9) J. Dhar, *Indian J. Phys.*, **7**, 43 (1932).
10) J. Trotter, *Acta Crystallogr.*, **14**, 1135 (1961).
11) G. B. Robertson, *Nature*, **191**, 593 (1961).
12) A. Hargreaves and S. H. Rizvi, *Acta Crystallogr.*, **15**, 365 (1962).
13) G. P. Charbonneau and Y. Delugeard, *Acta Crystallogr., Sect. B*, **33**, 1586 (1977).
14) H. M. Rietveld, E. N. Maslen, and C. J. B. Clews, *Acta Crystallogr., Sect. B*, **26**, 693 (1970).
15) J. L. Baudour and H. Cailleau, *Acta Crystallogr., Sect. B*, **33**, 1773 (1977).
16) Y. Delugeard, J. Desuche, and J. L. Baudour, *Acta Crystallogr., Sect. B*, **32**, 702 (1976).
17) H. Cailleau, J. L. Baudour, J. Meinnel, A. Dworkin, F. Moussa, and C. M. E. Zeyen, *Faraday Discuss. Chem. Soc.*, **69**, 7 (1980).
18) H. Cailleau and J. L. Baudour, *Acta Crystallogr., Sect. B*, **35**, 426 (1979).
19) J. L. Baudour and M. Sanquer, *Acta Crystallogr., Sect. B*, **39**, 75 (1983).
20) J. L. Baudour, Y. Delugeard, and H. Cailleau, *Acta Crystallogr., Sect. B*, **32**, 150 (1976).
21) J. L. Baudour, Y. Delugeard, and P. Rivet, *Acta Crystallogr., Sect. B*, **34**, 625 (1978).
22) T. Atake and H. Chihara, *Solid State Commun.*, **35**, 131 (1980).
23) K. Saito, T. Atake, and H. Chihara, *Bull. Chem. Soc. Jpn.*, **61**, 679 (1988).
24) H. Cailleau, "Incommensurate Phases in Dielectrics 2," ed by R. Blinc and A. P. Levanyuk, North-Holland,

Amsterdam (1985), Chap. 12.

25) S. S. Chang, *J. Chem. Phys.*, **79**, 6229 (1983).

26) K. Saito, T. Atake, and H. Chihara, *Bull. Chem. Soc. Jpn.*, **61**, 2327 (1988).

27) K. Saito, T. Atake, and H. Chihara, *J. Chem. Thermodyn.*, **17**, 539 (1985).

28) H. Cailleau, J. L. Baudour, A. Girard, and W. B. Yelon, *Solid State Commun.*, **20**, 577 (1976).

29) A. Girard, H. Cailleau, Y. Marqueton, and C. Ecolivet, *Chem. Phys. Lett.*, **54**, 479 (1978).

30) B. A. Bolton and P. N. Prasad, *Chem. Phys.*, **35**, 331 (1978).

31) H. Cailleau, A. Heidemann, and C. M. E. Zeyen, *J. Phys. C*, **12**, L411 (1979).

32) B. Toudic, J. Gallier, P. Rivet, and H. Cailleau, *Solid State Commun.*, **47**, 291 (1983).

33) R. E. Lechner, B. Toudic, and H. Cailleau, *J. Phys. C*, **17**, 405 (1984).

34) B. Toudic and R. E. Lechner, *J. Phys. C*, **17**, 5503 (1984).

35) T. Gullion, M. S. Conradi, and A. Rigamonti, *Phys. Rev. B*, **31**, 4388 (1985).

36) A. Girard, Y. Delugeard, L. Pichon, and B. Toudic, *J. Phys. I France*, **2**, 1833 (1992).

37) K. Saito, T. Atake, and H. Chihara, *J. Chem. Thermodyn.*, **18**, 407 (1986).

38) M. H. Lemee, L. Toupet, Y. Delugeard, J. C. Messager, and H. Cailleau, *Acta Crystallogr., Sect. B*, **43**, 466 (1987).

39) J. Wasicki, A. V. Belushkin, V. G. Khomenko, I. Natkaniec, Yu. V. Telezhenko, and T. Wasiutyński, *Phys. Status Solidi B*, **145**, 445 (1988).

40) K. Saito, T. Atake, and H. Chihara, *Acta Crystallogr., Sect. B*, **43**, 383 (1987).

41) "International Tables for X-Ray Crystallography," ed byJ. A. Ibers and W. C. Hamilton, Kynoch Press, Birmingham (1974), Vol. IV.

42) T. Sakurai and K. Kobayashi, "UNICS III," *Rep. Inst. Phys. Chem. Res.*, **55**, 69 (1979).

43) G. M. Sheldrick, "SHELXS-86, Program for the Solution of Crystal Structures," University of Göttingen, Germany (1986).

44) C. K. Johnson, "ORTEP II, Report ORNL-3794," Oak Ridge National Laboratory, Tennessee (1974).

45) The complete $|F_o|-\sigma(|F_o|)$ data, and the tables of anisotropic thermal parameters and molecular geometry obtained by the split atom analysis were deposited as Document No. 66040 at the Office of the Editor of Bull. Chem. Soc. Jpn.

46) Data collected on a crystal ($0.7\times0.5\times0.2$ mm^3). Crystal data: monoclinic, $P2_1/a$, $a=8.116(2)$, $b=5.613(1)$, $c=13.621(2)$ Å, $\beta=92.01(1)°$, $V=620.1(2)$ Å^3, $Z=2$, $\lambda(\text{Mo}\,K\alpha)=0.71069$ Å, R (non-split atom analysis)$=0.110$ and R (split atom analysis)$=0.098$ for 1142 reflections.

47) D. W. J. Cruickshank, *Acta Crystallogr.*, **9**, 757 (1956).

48) V. Shomaker and K. N. Trueblood, *Acta Crystallogr., Sect. B*, **24**, 63 (1968).

49) J. L. Baudour, *Acta Crystallogr., Sect. B*, **47**, 935 (1991).

50) Y. Onodera, *Prog. Theor. Phys.*, **44**, 1477 (1970).

51) Y. Onodera, *Prog. Theor. Phys.*, **45**, 986 (1971); **55**, 987 (1986).